SEMARAK ILMU PUBLISHING

Journal of Advanced Research in Micro and Nano Engineering

Journal homepage:
https://semarakilmu.com.my/journals/index.php/micro_nano_engineering/index
ISSN: 2756-8210

Insight into Magnesium Doping on Morphology, Optical, and Electrical Properties of Cu_2O Layer Synthesized by Electrodeposition Method

Nur Nisha Najjini Razalli[1], Mohd Zamzuri Mohamad Zain[1,*], Muhammad Mahyiddin Ramli[2], Marina Marzuki[2], Muhammad Hasnulhadi Jaafar[2], Fariza Mohamad[3], Pei Loon Khoo[4], Masanobu Izaki[4]

[1] Faculty of Mechanical Engineering Technology, Universiti Malaysia Perlis (UniMAP), Pauh Putra Campus, 02600 Arau, Perlis, Malaysia
[2] Faculty of Electronic Engineering Technology, Universiti Malaysia Perlis, Pauh Putra Main Campus, 02600, Arau, Perlis, Malaysia
[3] Faculty of Electrical & Electronic Engineering, University Tun Hussein Onn Malaysia, 86400, Parit Raja, Batu Pahat, Johor, Malaysia
[4] Department of Mechanical Eng., Toyohashi University of Technology, 1-1 Hibari Gaoka, Tempaku, Toyohashi, Aichi 441-8580, Japan

ARTICLE INFO

Article history:
Received 17 July 2024
Received in revised form 8 September 2024
Accepted 18 October 2024
Available online 30 November 2024

Keywords:
Mg doping; p-Cu_2O layer; electrodeposition; solar cell applications

ABSTRACT

Cu_2O stands out as a promising semiconductor material for solar energy conversion, primarily due to its exceptional light-absorbing qualities and its widespread availability. However, its efficiency is somewhat hindered by its relatively low carrier mobility and a limited absorption band for carriers. The introduction of magnesium (Mg) doping into Cu_2O has emerged as a potential means to enhance its morphology, optical characteristics, and electrical properties, making it an intriguing avenue for exploration. To fabricate the Mg-doped Cu_2O layers, an electrodeposition process was employed on an Indium Tin Oxide (ITO) substrate. The resulting films were then subjected to characterization using Field Emission Scanning Electron Microscopy (FESEM), Ultraviolet-Visible Spectroscopy (UV-Vis), and HALL Effect Measurement, focusing on their morphology, optical properties, and electrical behaviors. Notably, the concentration of magnesium played a significant role in shaping the properties of the Cu_2O layer. The fabrication process extended up to a dopant concentration of 0.3 M for both undoped Cu_2O and Mg-doped Cu_2O layers, leading to morphological alterations. Specifically, the grain size increased with varying dopant concentrations, but it became smaller and more compact after doping with 0.3 M Mg. The average absorbance of visible light for both undoped and Mg-doped Cu_2O layers fell within the range of 1~2 au. Intriguingly, a doping level of 0.3 M Mg led to the simultaneous achievement of high carrier mobility (29.98 cm^2/Vs), low bulk carrier concentration (2.3.928 x 10^{21} cm^{-3}), and high resistivity (5.3 x 10^{-5} Ω cm) in the Cu_2O material. Additionally, Cu_2O/ITO thin films exhibiting rectifying characteristics were successfully fabricated, confirming the semiconductor nature of the deposited p-type Cu_2O layer. The primary objective of this study was to synthesize Cu_2O layers doped with varying concentrations of Mg and thoroughly characterize their morphology, optical attributes, and electrical behaviors through the electrodeposition method. The study findings and implications were extensively discussed.

1. Introduction

* *Corresponding author.*
E-mail address: mzamzuri@unimap.edu.my

https://doi.org/10.37934/armne.27.1.7687

The concept of "all-oxide photovoltaics" is attracting significant attention and interest, primarily due to the cost-effectiveness, abundance, and long-term stability associated with devices based on metal oxides. Generally, metal oxides are characterized by wide band gaps and transparency, which make them less favorable for use as the absorber material in solar cells, with limited absorption primarily in the UV region. However, there is a notable exception among oxides, which is copper oxide. Copper oxide exists in three distinct phases: cuprous oxide (Cu_2O) also known as cuprite), cupric oxide (CuO, or tenorite), and Cu_4O_3 (referred to as paramelaconite) [1,2]. Among these phases, the first two, cuprous oxide (Cu_2O) and cupric oxide (CuO), have been the primary focus of analysis and research for their potential applications in photovoltaic devices. Cuprous oxide (Cu_2O) is regarded as a promising p-type semiconductor material in photovoltaics, photocatalysis, and optoelectronics due to its stability, ease of preparation, abundance in nature, non-toxicity, and visible-light activity with a direct bandgap of 2.0~2.6 eV [3-5].

Copper oxide thin films have been successfully fabricated through a variety of physical and chemical processes, which include nebulizer pyrolysis [6], thermal oxidation of copper sheets [7], magnetron sputtering [8,9], spin coating [10], and more recently, the electrodeposition method [11-13]. Among these methods, electrochemical deposition stands out as one of the most fundamental and cost-effective techniques. It is highly adaptable and particularly efficient for large-area device production [14]. What further enhances the appeal of electrodeposition is the ability to fine-tune electrochemical parameters and the composition of the electrolytic solution. Also, electrodeposition can control to produce the well dispersed Cu_2O deposition due to Cu_2O provide a conductive pathway for electrons, enabling them to move more freely through the material [15]. This fine control offers significant advantages in regulating the film's thickness, morphology, and characteristics, making electrodeposition a particularly attractive choice. Moreover, it is worth noting that by adjusting various electrodeposition parameters, it is possible to produce single-phase Cu_2O layers with precision [16].

Additionally, the smaller grain size observed in Cu_2O oxide layers can have an impact on electron transport, potentially leading to recombination losses before an electron enters the excited state. This, in turn, directly reduces the efficiency of photovoltaic devices [17]. Cu_2O (cuprous oxide) presents several attractive features, including non-toxicity, abundance of its constituent elements, cost-effective production, and a direct band gap, making it a promising material for use as a p-type Transparent Conductive Oxide (TCO). Notably, Cu_2O exhibits relatively respectable hole mobility values, falling within the range of 101-102 $cm^2V^{-1}s^{-1}$ [18]. Its native p-type conductivity is attributed to the introduction of acceptor states in the material's band gap due to copper vacancies [19].

However, current Cu_2O layer materials have certain limitations in their optical and electrical properties. Specifically, they tend to exhibit relatively high resistivity, typically exceeding 102 Ωcm, and possess a relatively low band gap energy, which is approximately 2.17 eV, restricting their optical performance [20]. Moreover, studies have shown that doping Cu_2O layers with various elements can significantly enhance electrical conductivity along the interface. This enhancement occurs not by increasing the concentration of charge carriers but by boosting their mobility, as reported by Lachinov. Additionally, doping can alter the microstructure of the oxide layer, offering opportunities to fine-tune its properties [21,22]. Furthermore, incorporating insolvent dopants into cuprous oxide in thin-film solar cells has the potential to adjust its energy band gap and modify the microstructure of the oxide layer [23-25].

To further enhance the properties of Cu_2O, various doping elements like nitrogen [24], lithium [25], chlorine [26], and fluorine [27] can be introduced. Additionally, ab initio calculations conducted by Nolan and Elliot suggest that doping with larger cations, such as Mg^{2+}, Sr^{2+}, Zn^{2+}, Ga^{3+}, or Sn^{2+}, can

lead to improvements in both transparency and conductivity [28]. This doping mechanism may also raise the band gap value, meeting the requirements for transparent electronics applications while maintaining a high level of p-type conductivity. In recent developments, Resende *et al.,* [29] achieved the incorporation of Mg into Cu_2O using chemical vapor deposition (CVD) processes. Their findings indicated a significant reduction in electrical resistivity, reaching as low as 6.6 Ωcm, along with a slight enhancement in transmittance in the visible wavelength range, which reached up to 51%.

In our study, we delve into the functional characteristics of both undoped and Mg-doped Cu_2O oxide layers, employing various doping concentrations through the electrodeposition method. By harnessing a comprehensive array of dedicated characterization techniques, we conduct an extensive examination of the morphology, optical attributes, and electrical behaviors of these films. This thorough analysis involves the use of Field Emission Scanning Electron Microscopy (FESEM), Ultraviolet-Visible Spectroscopy (UV-Vis), and HALL Effect measurement. Our research underscores the critical significance of controlling the deposition parameters related to doping concentrations. This control proves essential in attaining the optimal physical properties of these oxide layers.

2. Methodology

2.1 Preparation of ITO Substrate Glass

For the substrate, we selected an ITO glass with a resistance of approximately 10 mΩ, possessing dimensions of 2 cm in length, 1 cm in width, and 0.75 mm in thickness (l x w x t). Before commencing the electrodeposition procedure, we partitioned the ITO glass into two distinct areas: the region designated for deposition and the non-deposited area. Subsequently, it was immersed in acetone for approximately 2 minutes. Following this step, the glass substrate was thoroughly rinsed with deionized water and subsequently dried using pressurized air.

2.2 Electrodeposition of Undoped Cu_2O and Mg Doped Cu_2O Oxide Layers

The electrodeposition of Cu_2O oxide layers was carried out using a two-electrode setup, where a Pt wire served as the counter electrode and an ITO substrate glass served as the working electrode. To maintain stability, a platinum wire was employed as the anode since it doesn't undergo oxidation when used as a cathode. The Cu_2O electrolyte solution was prepared by dissolving 79.86 g of 99% pure copper (II) acetate monohydrate ($C_4H_{10}CuO_6$) from Kanto Chemical Co., Inc., along with 270.24 g of 85~92% pure lactic acid ($C_3H_6O_6$) from the same supplier, and 210 g of potassium hydroxide (KOH) with a chemical purity of 86% into 500 ml of ultrapure water (UPW) at ambient temperature. It's worth noting that all aqueous solutions used were meticulously prepared using a water purification system, specifically the Milli-Q IQ 7003. The pH of the solution was adjusted to 12.5 by the addition of KOH. The deposition parameters employed in the electrodeposition process are detailed in Table 1. In the case of the starting solution for Mg-doped Cu_2O oxide layers, 95% pure magnesium hydroxide from Acros Organics was utilized to formulate doping concentrations of 0.1 M, 0.2 M, and 0.3 M Mg in Cu_2O.

Table 1
Electrodeposition parameters of undoped Cu_2O and Mg doped Cu_2O

Deposition parameters	
Current (mA)	2.0
Voltage (V)	1.0
Bath temperature (^oC)	45.5
Solution temperature (^oC)	40.0
pH value	12.5
Deposition time (min)	3.0

2.3 Characterization of Analysis

The morphology of undoped Cu_2O and Mg doped Cu_2O on ITO glass substrate was observed by FESEM (Leo 1525) with 20x to 70x magnification and 7 kV of accelerating voltage. Next, the optical properties of thin films were observed by UV-Vis (Perkin ELMER LAMBDA 950 Series) in the wavelength range of 200-800 µm referenced to the air. For electrical properties of the thin film were observed by HALL Effect Measurement (ECOPIA HT55T3) with a current of 5 mA, and a diameter of 0.1 µm to measure the carrier concentration, mobility carrier, and resistivity.

3. Results

3.1 The Appearance of Undoped Cu_2O and Mg Doped Cu_2O Thin Films

Figure 1 provides a schematic illustration of the deposition of Mg-doped Cu_2O on the ITO substrate. The Cu_2O layer was applied to the ITO substrate, with varying concentrations of 0.1 M, 0.2 M, and 0.3 M Mg. In Figure 2, you can observe the physical appearance of the Cu_2O layer before and after doping with different concentrations of Mg. The initially clear color of the ITO substrate transforms into a consistent light brown hue after being coated with both undoped Cu_2O and Mg-doped Cu_2O. Interestingly, there are no distinct visual changes in the appearance of the Cu_2O layers when different Mg doping concentrations are applied.

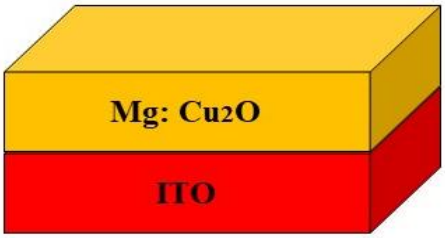

Fig. 1. Illustration cell configuration of Mg doped Cu_2O on ITO substrate glass

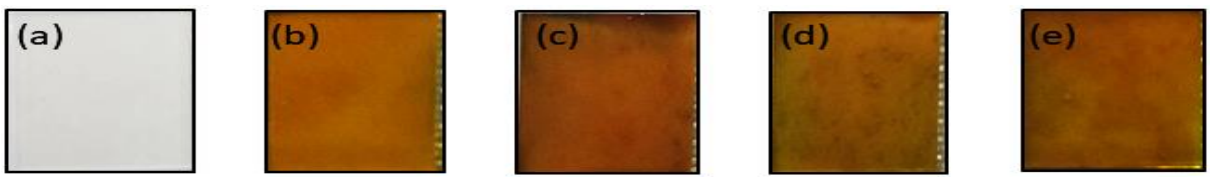

Fig. 2. The appearance of Cu_2O (a) ITO substrate glass (b) Undoped (c) 0.1 M (d) 0.2 M (e) 0.3 M Mg doped Cu_2O

3.2 Surface Morphology of Undoped Cu_2O and Mg Doped Cu_2O Oxide Layers

Figure 3 provides a detailed view of the morphology of both undoped and Mg-doped Cu_2O oxide layers, each featuring varying dopant concentrations. The Cu_2O grains exhibit a pyramid-like structure [30], forming a consistently uniform and compact layer, regardless of the doping concentration, when deposited at 1 V and 2 mA. However, it's noteworthy that the distribution of grain sizes undergoes changes depending on the Mg doping concentration applied. For instance, the grain size increases for concentrations of 0.1 M and 0.2 M, while the sample doped with 0.3 M Mg exhibits notable differences in surface morphology and grain size. Figure 3(d) clearly illustrates that the grain size has decreased compared to the other samples. Figure 4 provides a quantitative comparison of the grain sizes for undoped Cu_2O and Mg-doped Cu_2O oxide layers.

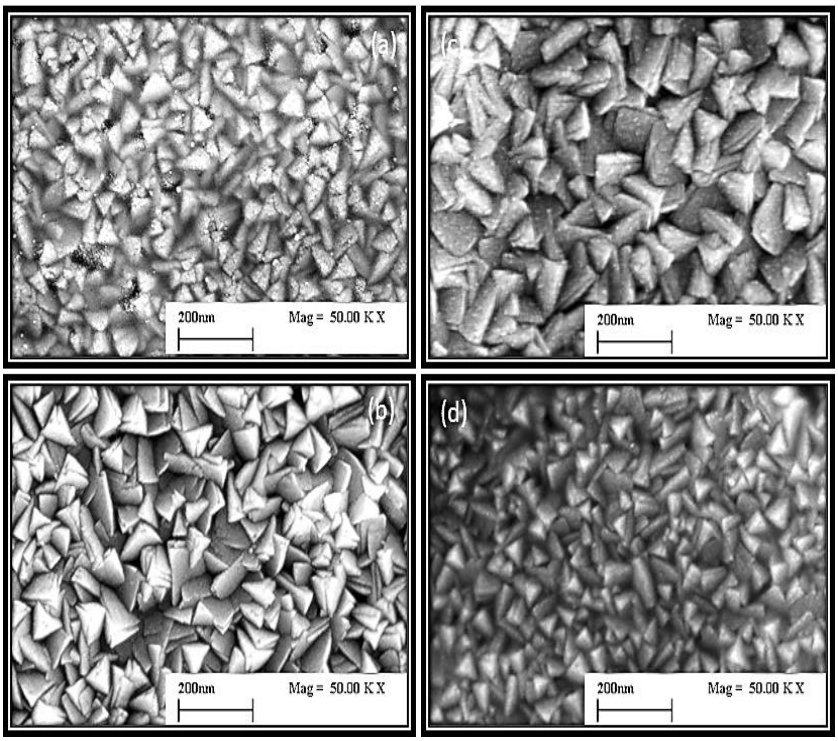

Fig. 3. Morphology structure of (a) undoped, (b) 0.1 M, (c) 0.2 M, and (d) 0.3 M Mg doped Cu_2O

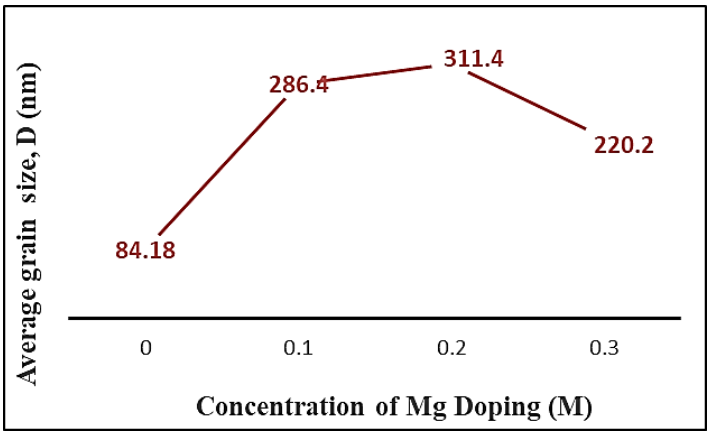

Fig. 4. Average grain size of undoped, and Mg doped Cu_2O with different concentrations

The undoped sample has an average grain size of 84.18 nm, as shown in Figure 4. In contrast, the introduction of 0.1 M Mg doping into Cu_2O leads to an increase in grain size, resulting in an average size of 286.4 nm. The 0.2 M Mg-doped Cu_2O oxide layer exhibits an even larger average grain size of 311.4 nm. However, when doping with 0.3 M Mg, the grain size decreases to 220.2 nm, as evidenced in Figure 3(d). This decrease is attributed to the stress within the grains, which alters the grain structure after Mg doping in Cu_2O layers [31].

3.3 Optical Analysis of Undoped Cu_2O and Mg Doped Cu_2O Oxide Layers

Figure 5 presents the absorption spectrum of Cu_2O oxide layers doped with Mg at varying concentrations. The absorption spectrum was measured within the range of 300 to 800 nm at room temperature. The results clearly demonstrate that higher absorption bands are achieved after the introduction of Mg doping, regardless of the specific doping concentration. Notably, the absorption edge, occurring at a wavelength of 500 nm, exhibits the highest absorption band for the Cu_2O layer doped with 0.2 M Mg, reaching its peak. In contrast, the Cu_2O oxide layer doped with 0.3 M Mg shows an absorbance of approximately 1 au in the visible light range. It's important to recognize that the absorption profile is influenced by various factors, including lattice strain, film thickness, oxygen availability, and particle size within the samples [32]. The observed changes in the absorption profile in our study can be attributed to the lattice strain induced in the structure after the introduction of Mg doping. While Mg^{2+} and Cu^{+} have similar ionic radii, leading to minimal structural distortion that doesn't significantly disturb Cu-Cu interactions [33], there are still subtle differences in the optical band gap. These differences can be attributed to the lattice strain induced by the Mg doping concentration, ultimately affecting the absorption profile.

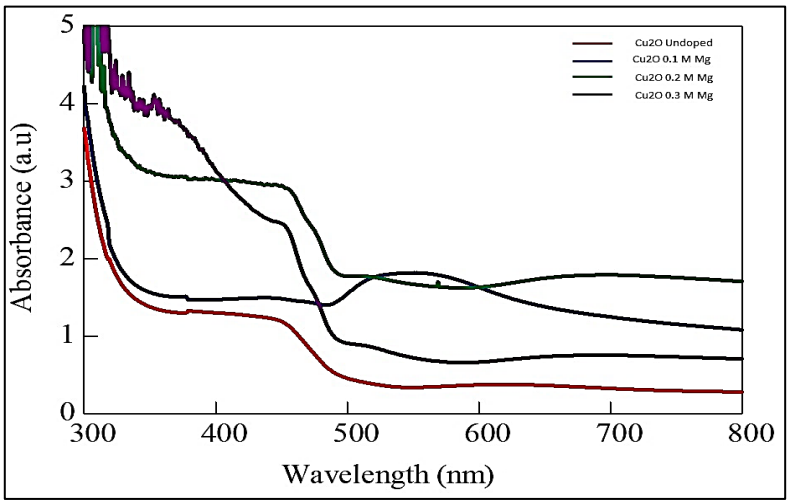

Fig. 5. Absorption spectrum of undoped and Mg doped Cu_2O with different concentrations

3.4 Electrical Analysis of Undoped and Mg Doped Cu_2O Oxide Layers

The carrier concentration, mobility carrier, and resistivity of electrodeposited undoped and Mg-doped Cu_2O oxide layers were analyzed by using the HALL Effect measurement. Table 2 shows the result of the HALL Effect measurement of the undoped and Mg-doped Cu_2O.

Table 2
Analysis result of HALL effect measurement of the undoped and Mg doped Cu_2O

Concentration of Mg doping (M)	Carrier concentration x 10^{21} (/cm^3)	Mobility carrier x 10 (cm^2/vs)	Resistivity x 10^{-5} (Ωcm)
Undoped	3.021	3.556	5.829
0.1	3.344	3.115	5.993
0.2	2.596	4.022	5.980
0.3	3.928	2.998	5.300

3.4.1 Bulk carrier concentration analysis of undoped and Mg doped Cu_2O oxide layers

Figure 6 displays a graph illustrating the bulk concentration (/cm^3) in relation to the concentration of Mg doping (M). Interestingly, the graph does not exhibit a discernible trend as the dopant is progressively added to the Cu_2O oxide layers. For the Cu_2O oxide layer doped with 0.1 M Mg, the bulk concentration increases from 3.012 x 10^{21} to 3.344 x 10^{21} cm^{-3}. However, when the Mg concentration is increased to a 0.2 M Mg-doped Cu_2O oxide layer, the bulk concentration takes a dip, reaching its lowest value of 2.596 x 10^{21} cm^{-3}. This decrease is likely influenced by the larger grain sizes observed, which result in gaps or voids between the grains. Smaller crystallite sizes and a higher density of grain boundaries act as barriers for carrier transport and trap free carriers, contributing to this reduction [32]. Conversely, in the case of the 0.3 M Mg-doped Cu_2O oxide layer, which exhibits a more compact structure, the bulk concentration increases to its highest value of 3.928 x 10^{21} cm^{-3}. This phenomenon can be attributed to the doping process, which introduces an acceptor level slightly higher than the valence band in the band structure. This acceptor level receives electrons (e^-) transitioning from the valence band, leading to the formation of electron holes (h^+) in the valence band. This process ultimately results in a higher carrier concentration according to the previous study [34].

In comparison to previous research efforts, where Mg-doped Cu_2O oxide layer was fabricated using various techniques, the results of our study reveal a notable enhancement in carrier concentration. For instance, Prabu *et al.*, [35] conducted research employing a nebulizer spray pyrolysis technique with different pressure rates. In their work, the highest carrier concentration was achieved at a pressure of 3 bars, with a carrier concentration value of 17.60 x 10^{15} cm^{-3}. Similarly, Joao *et al.,* [29] undertook research on Mg-doped Cu_2O, utilizing aerosol-assisted metal-organic chemical vapor deposition. Their findings indicated that incorporating magnesium doping led to an increase in charge carrier density (holes) of up to 8.1 x 10^{17} cm^{-3}. This effect was attributed to the increase in simple copper vacancies resulting from the presence of magnesium in a tetrahedral position, consequently raising the hole concentration, as proposed by Nolan *et al.,* [28].

When comparing these findings to our research, it becomes evident that Mg-doped Cu_2O oxide layers fabricated in our study exhibit superior carrier concentration. Specifically, the highest carrier concentration was attained in the 0.3 M Mg-doped Cu_2O oxide layer, with a value of 3.928 x 10^{21} cm^{-3}. This highlights the significant enhancement in carrier concentration achieved in our Mg-doped Cu_2O oxide layers compared to previous studies.

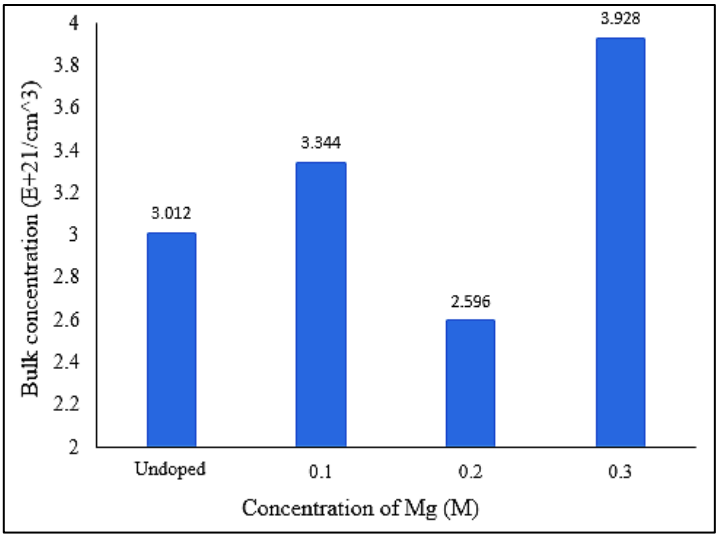

Fig. 6. Bulk concentration measurement of undoped and Mg doped Cu_2O oxide layers

3.4.2 Mobility carrier analysis of undoped and Mg doped Cu_2O oxide layers

Figure 7 illustrates the relationship between carrier mobility (cm^2/Vs) and the concentration of Mg doping (M). In our study, for the 0.1 M and 0.3 M Mg-doped Cu_2O oxide layers, carrier mobility decreases from 3.556 x 10 cm^2/Vs for undoped Cu_2O to 3.115 x 10 cm^2/Vs for 0.1 M, and further reduces to its lowest value of 2.998 x 10 cm^2/Vs for 0.3 M doping. This trend aligns with findings from previous research, indicating that as doping concentration increases, carrier mobility tends to decrease. The explanation for this phenomenon lies in the concept that electrons or holes can only move freely under the influence of an electric field when they are mobile. When doping levels increase, the concentration of charge carriers rises, which, in turn, increases the likelihood of charge carrier collisions. These collisions subsequently lead to a reduction in carrier mobility [36]. Interestingly, for the 0.2 M Mg-doped Cu_2O oxide layer, carrier mobility shows an opposite trend. It increases from 3.556 x 10 cm^2/Vs for the undoped Cu_2O oxide layer to its highest mobility value of 4.022 x 10 cm^2/Vs. This result can be explained by the lower value of carrier concentration in this sample. With less carrier (holes) present, as indicated in the carrier concentration analysis, the high mobility observed for the 0.2 M Mg-doped Cu_2O oxide layer is consistent with this lower carrier concentration.

To provide a comparison, research by Naama *et al*., [37] which focused on Mg-doped Cu_2O oxide layers fabricated using magnetron sputtering under optimized pressure conditions, found that the mobility decreased from 8.31 cm^2/Vs to 0.11 cm^2/Vs with the incorporation of Mg. This comparison suggests that the Mg-doped Cu_2O oxide layers produced via electrodeposition in our experiment exhibits superior mobility characteristics. Even after adding Mg dopant, the mobility remains relatively higher, with the lowest mobility recorded at 0.3 M Mg-doped Cu_2O oxide layer, where it reaches a value of 2.998 x 10 cm^2/Vs.

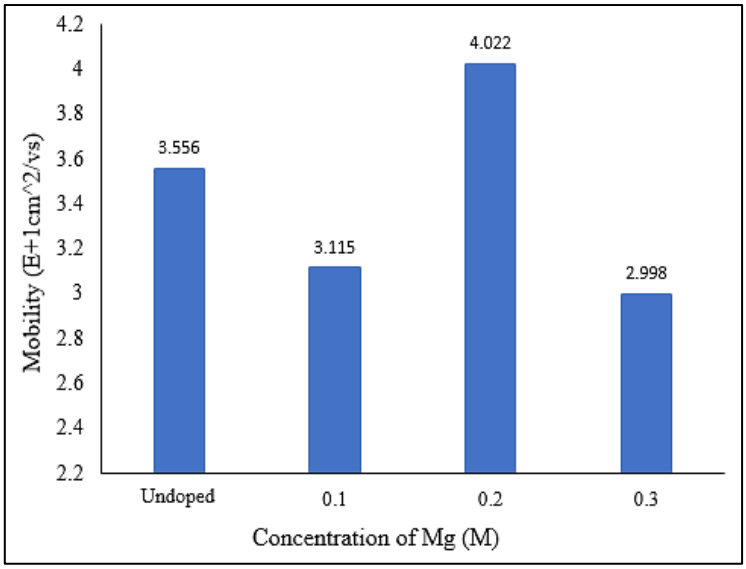

Fig. 7. Mobility carrier of undoped and Mg doped Cu_2O oxide layers

3.4.3 Resistivity analysis of undoped and Mg doped Cu_2O oxide layers

Figure 8 presents the graph depicting resistivity (Ω·cm) as a function of Mg doping concentration (M). Interestingly, there is no discernible pattern that can be conclusively established. For the 0.1 M Mg-doped Cu_2O oxide layer, resistivity experiences a slight increase, rising from 5.829 x 10^{-5} Ω·cm to 5.993 x 10^{-5} Ω·cm. A similar trend is observed for the 0.2 M Mg-doped Cu_2O oxide layer, where resistivity decreases slightly from 5.993 x 10^{-5} Ω·cm to 5.980 x 10^{-5} Ω·cm, albeit it remains somewhat higher than the resistivity value of undoped Cu_2O oxide layer. This increase in resistivity following doping at 0.1 M and 0.2 M may be attributed to the introduction of carrier traps by the doping process, which in turn limits the movement of carriers. However, a distinct shift occurs as the doping concentration is increased to 0.3 M Mg-doped Cu_2O oxide layer, where the resistivity significantly drops to 5.300 x 10^{-5} Ω·cm. This reduction in resistivity can be attributed to the increased Cu voltage density resulting from the incorporation of Mg^{2+} ions into the Cu_2O lattice, which contributes to a reduction in electrical resistance caused by Mg doping [38].

For the sake of comparison, research by Santhosh *et al*., [39] involving Mg-doped Cu_2O oxide layers prepared using the nebulizer pyrolysis technique, showed that at a 7% Mg doping concentration, Cu_2O resistivity reached its lowest point at 1.53×10^2 Ω·cm. This demonstrates that the incorporation of Mg dopant into Cu_2O leads to decreased resistivity and improved conductivity. Additionally, our research outperforms this previous work, with the most optimal resistivity obtained at 0.3 M Mg-doped Cu_2O oxide layer, measuring 5.300 x 10^{-5} Ω·cm, which is approximately 7 times better.

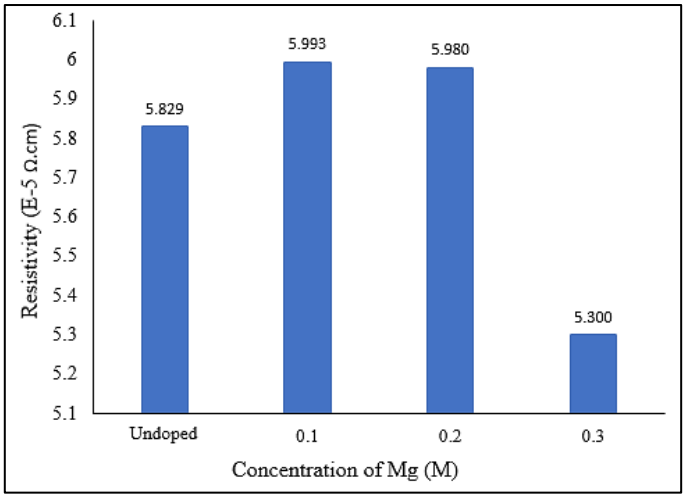

Fig. 8. Resistivity of undoped and Mg doped Cu_2O oxide layers from HALL effect measurement

4. Conclusions

In summary, our study successfully fabricated undoped Cu_2O and Mg-doped Cu_2O oxide layers using the electrodeposition method on ITO substrates. The impact of Mg doping concentration on morphology, optical and electrical properties of these samples have been investigated. The electrodeposition process was carried out in an alkaline aqueous solution containing copper (II) acetate and lactic acid. The observation of the Cu_2O oxide layers via Field Emission Scanning Electron Microscopy (FESEM) revealed that they possess a pyramid-like structure and exhibit a polycrystalline nature. The change in grain size of the Cu_2O structure was observed as the Mg concentration increased, attributed to the stress present within the crystals after doping. The average absorbance of visible light ranged from 1 to 2 au. The Hall Effect measurements indicated that Mg-doped Cu_2O oxide layers effectively enhanced the electrical characteristics of Cu_2O at specific doping concentrations, including improvements in bulk concentration, bulk mobility, and resistivity. Notably, the 0.3 M Mg-doped Cu_2O oxide layer exhibited superior electrical properties, with a bulk concentration of 3.928×10^{21} cm^{-3} and a resistivity of 5.300×10^{-5} Ω·cm.

Acknowledgement

The author gratefully acknowledges the financial support provided by the Malaysian Ministry of Higher (MOE) through the Fundamental Research Grant Scheme (FRGS) under Grant No. FRGS/1/2019/TK07/UNIMAP/02/2.

References

[1] Meyer, B. K., Angelika Polity, D. Reppin, Martin Becker, P. Hering, P. J. Klar, Th Sander, C. Reindl, J. Benz, M. Eickhoff, C. Heiliger, M. Heinemann, J. Bläsing, A. Krost, S. Shokovets, C. Müller, C. Ronning. "Binary copper oxide semiconductors: From materials towards devices." *Physica Status Solidi (b)* 249, no. 8 (2012): 1487-1509. https://doi.org/10.1002/pssb.201248128

[2] Sun, Zhe, Ruixue Cao, Manhong Huang, Donghui Chen, Wei Zheng, and Li Lin. "Effect of light irradiation on the photoelectricity performance of microbial fuel cell with a copper oxide nanowire photocathode." *Journal of Photochemistry and Photobiology A: Chemistry* 300 (2015): 38-43. https://doi.org/10.1016/j.jphotochem.2014.12.003

[3] Zainal, S. M., M. Zamzuri, M. Hasnulhadi, Z. Nooraizedfiza, M. Marina, Fariza Mohamad, N. Hisyamudin, and M. Izaki. "Effect of annealing temperature on construction of CuO layer on electrodeposited-Cu_2O layer by annealing." In *IOP Conference Series: Materials Science and Engineering*, 429, no. 1, p. 012097. IOP Publishing, 2018. https://doi.org/10.1088/1757-899X/429/1/012097

[4] Zhao, Ying-jie, Yan Li, Yong-bin Wu, Wei Zhou, and Fu-xin Zhong. "Preparation and photoelectric properties of praseodymium-doped cuprous oxide thin films." *Journal of Materials Science: Materials in Electronics* 31 (2020): 3092-3100. https://doi.org/10.1007/s10854-020-02855-4

[5] Yue, Yamei, Pengxin Zhang, Wei Wang, Yuncheng Cai, Fatang Tan, Xinyun Wang, Xueliang Qiao, and Po Keung Wong. "Enhanced dark adsorption and visible-light-driven photocatalytic properties of narrower-band-gap Cu2S decorated Cu2O nanocomposites for efficient removal of organic pollutants." *Journal of Hazardous Materials* 384 (2020): 121302. https://doi.org/10.1016/j.jhazmat.2019.121302

[6] Jacob, S. Santhosh Kumar, I. Kulandaisamy, S. Valanarasu, A. M. S. Arulanantham, V. Ganesh, S. AlFaify, and A. Kathalingam. "Enhanced optoelectronic properties of Mg doped Cu 2 O thin films prepared by nebulizer pyrolysis technique." *Journal of Materials Science: Materials in Electronics* 30 (2019): 10532-10542. https://doi.org/10.1007/s10854-019-01397-8

[7] Mittiga, Alberto, Enrico Salza, Francesca Sarto, Mario Tucci, and Rajaraman Vasanthi. "Heterojunction solar cell with 2% efficiency based on a Cu_2O substrate." *Applied Physics Letters* 88, no. 16 (2006). https://doi.org/10.1063/1.2194315

[8] Noda, S., H. Shima, and H. Akinaga. "Cu_2O/ZnO heterojunction solar cells fabricated by magnetron-sputter deposition method films using sintered ceramics targets." In *Journal of Physics: Conference Series*, 433, no. 1, p. 012027. IOP Publishing, 2013. https://doi.org/10.1088/1742-6596/433/1/012027

[9] Zamzuri, M., H. Jaafar, N. Rosli, M. Mat Salleh, N. Tajul Lile, M. Azaman, F. Mohamad, N. Hisyamudin, and M. Izaki. "Sputtered AZO on< 111>-oriented Cu_2O photovoltaic device with improved performance." In *IOP Conference Series: Materials Science and Engineering*, 226, no. 1, p. 012178. IOP Publishing, 2017. https://doi.org/10.1088/1757-899X/226/1/012178

[10] Oku, Takeo, Tetsuya Yamada, Kazuya Fujimoto, and Tsuyoshi Akiyama. "Microstructures and photovoltaic properties of Zn (Al) O/Cu_2O-based solar cells prepared by spin-coating and electrodeposition." *Coatings* 4, no. 2 (2014): 203-213. https://doi.org/10.3390/coatings4020203

[11] Hussain, Sajad, Chuanbao Cao, Ghulam Nabi, Waheed S. Khan, Zahid Usman, and Tariq Mahmood. "Effect of electrodeposition and annealing of ZnO on optical and photovoltaic properties of the p-Cu_2O/n-ZnO solar cells." *Electrochimica Acta* 56, no. 24 (2011): 8342-8346. https://doi.org/10.1016/j.electacta.2011.07.017

[12] Wijesundera, R. P. "Fabrication of the CuO/Cu_2O heterojunction using an electrodeposition technique for solar cell applications." *Semiconductor Science and Technology* 25, no. 4 (2010): 045015. https://doi.org/10.1088/0268-1242/25/4/045015

[13] Zamzuri, Mohd, Junji Sasano, Fariza Binti Mohamad, and Masanobu Izaki. "Substrate type< 111>-Cu2O/< 0001>-ZnO photovoltaic device prepared by photo-assisted electrodeposition." *Thin Solid Films* 595 (2015): 136-141. https://doi.org/10.1016/j.tsf.2015.10.054

[14] Tran, Man Hieu, Jae Yu Cho, Soumyadeep Sinha, Myeng Gil Gang, and Jaeyeong Heo. "Cu_2O/ZnO heterojunction thin-film solar cells: the effect of electrodeposition condition and thickness of Cu_2O." *Thin Solid Films* 661 (2018): 132-136. https://doi.org/10.1016/j.tsf.2018.07.023

[15] Alias, Muhammad Afiff, Khairul Fadzli Samat, Nuraiham Mohamed, Mohd Warikh Abd Rashid, Mohd Asyadi Azam, Nguyen Van Toan, Takahito Ono, Alicja Klimkowicz, and Akito Takasaki. "Electrodeposited bismuth telluride nanocomposite thermoelectric film with improved graphene deposition." *Journal of Advanced Research in Applied Mechanics* 111, no. 1 (2023): 161-172. https://doi.org/10.37934/aram.111.1.161172

[16] Messaoudi, Olfa, Sarra Elgharbi, Amira Bougoffa, Moufida Mansouri, Afrah Bardaoui, Safa Teka, Leila Manai, and Arwa Azhary. "Annealing temperature investigation on electrodeposited Cu_2O properties." *Phase Transitions* 93, no. 10-11 (2020): 1089-1099. https://doi.org/10.1080/01411594.2020.1837379

[17] Zang, Zhigang. "Efficiency enhancement of ZnO/Cu_2O solar cells with well oriented and micrometer grain sized Cu2O films." *Applied Physics Letters* 112, no. 4 (2018). https://doi.org/10.1063/1.5017002

[18] Al-Jawhari, H. A. "A review of recent advances in transparent p-type Cu_2O-based thin film transistors." *Materials Science in Semiconductor Processing* 40 (2015): 241-252. https://doi.org/10.1016/j.mssp.2015.06.063

[19] Scanlon, David O., Benjamin J. Morgan, Graeme W. Watson, and Aron Walsh. "Acceptor levels in p-type Cu 2 O: rationalizing theory and experiment." *Physical Review Letters* 103, no. 9 (2009): 096405. https://doi.org/10.1103/PhysRevLett.103.096405

[20] Ghijsen, Jacques, Liu-Hao Tjeng, Jan van Elp, Henk Eskes, Jos Westerink, George A. Sawatzky, and Marek T. Czyzyk. "Electronic structure of Cu_2O and CuO." *Physical Review B* 38, no. 16 (1988): 11322. https://doi.org/10.1103/PhysRevB.38.11322

[21] Senthil, T. S., N. Muthukumarasamy, and Misook Kang. "Improved performance of ZnO thin film solar cells by doping magnesium ions." *Journal of Materials Science: Materials in Electronics* 24 (2013): 3963-3969. https://doi.org/10.1007/s10854-013-1348-2

[22] Rana, N., Subhash Chand, and Arvind K. Gathania. "Band gap engineering of ZnO by doping with Mg." *Physica Scripta* 90, no. 8 (2015): 085502. https://doi.org/10.1088/0031-8949/90/8/085502
[23] Bergerot, Laurent, Carmen Jiménez, Odette Chaix-Pluchery, Laetitia Rapenne, and Jean-Luc Deschanvres. "Growth and characterization of Sr-doped Cu_2O thin films deposited by metalorganic chemical vapor deposition." *Physica Status Solidi (a)* 212, no. 8 (2015): 1735-1741. https://doi.org/10.1002/pssa.201431750
[24] Ye, Fan, Jun-Jie Zeng, Yi-Bin Qiu, Xing-Min Cai, Bo Wang, Huan Wang, Dong-Ping Zhang, Ping Fan, Yi-Zhu Xie, Xiu-Fang Ma, and Fan Wang. "The optical and electrical properties of nitrogen-doped cuprous oxide annealed at different temperatures." *Surface and Coatings Technology* 359 (2019): 360-365. https://doi.org/10.1016/j.surfcoat.2018.12.109
[25] Cho, Kyung-Su, Doo-Hee Kim, Young-Hwan Kim, Junghyo Nah, and Han-Ki Kim. "Li-doped Cu_2O/ZnO heterojunction for flexible and semi-transparent piezoelectric nanogenerators." *Ceramics International* 43, no. 2 (2017): 2279-2287. https://doi.org/10.1016/j.ceramint.2016.10.208
[26] Pelegrini, Silvia, Milton André Tumelero, Iuri Stefani Brandt, Rafael Domingues Della Pace, Ricardo Faccio, and Andre Avelino Pasa. "Electrodeposited Cu_2O doped with Cl: Electrical and optical properties." *Journal of Applied Physics* 123, no. 16 (2018). https://doi.org/10.1063/1.5004782
[27] Yu, Luo, Liangbin Xiong, and Ying Yu. "Cu_2O homojunction solar cells: F-doped N-type thin film and highly improved efficiency." *The Journal of Physical Chemistry C* 119, no. 40 (2015): 22803-22811. https://doi.org/10.1021/acs.jpcc.5b06736
[28] Nolan, Michael, and Simon D. Elliott. "Tuning the transparency of Cu2O with substitutional cation doping." *Chemistry of Materials* 20, no. 17 (2008): 5522-5531. https://doi.org/10.1021/cm703395k
[29] Resende, João, Carmen Jiménez, Ngoc Duy Nguyen, and Jean-Luc Deschanvres. "Magnesium-doped cuprous oxide (Mg: Cu2O) thin films as a transparent p-type semiconductor." *Physica Status Solidi (a)* 213, no. 9 (2016): 2296-2302. https://doi.org/10.1002/pssa.201532870
[30] Zamzuri, Mohd, Junji Sasano, Fariza Binti Mohamad, and Masanobu Izaki. "Substrate type< 111>-Cu2O/< 0001>-ZnO photovoltaic device prepared by photo-assisted electrodeposition." *Thin Solid Films* 595 (2015): 136-141. https://doi.org/10.1016/j.tsf.2015.10.054
[31] Yuan, Binxia, Xiaobo Liu, Xiaodong Cai, Xinyi Fang, Jianfeng Liu, Maoliang Wu, and Qunzhi Zhu. "Preparation of zinc and cerium or both doped Cu_2O photoelectric material via hydrothermal method." *Solar Energy* 196 (2020): 74-79. https://doi.org/10.1016/j.solener.2019.11.093
[32] Yathisha, R. O., and Y. Arthoba Nayaka. "Structural, optical and electrical properties of zinc incorporated copper oxide nanoparticles: doping effect of Zn." *Journal of Materials Science* 53 (2018): 678-691. https://doi.org/10.1007/s10853-017-1496-5
[33] Kardarian, Kasra, Daniela Nunes, Paolo Maria Sberna, Adam Ginsburg, David A. Keller, Joana Vaz Pinto, Jonas Deuermeier, Assaf Y. Anderson, Arie Zaban, Rodrigo Martins, Elvira Fortunato. "Effect of Mg doping on Cu_2O thin films and their behavior on the TiO2/Cu_2O heterojunction solar cells." *Solar Energy Materials and Solar Cells* 147 (2016): 27-36. https://doi.org/10.1016/j.solmat.2015.11.041
[34] Lin, Shih-Hung, Rong-Hwei Yeh, Chen Chu, and Ruei-Sung Yu. "Effects of Mg doping on structural and optoelectronic properties of p-type semiconductor CuCrO2 thin films." *Materials Science in Semiconductor Processing* 139 (2022): 106346. https://doi.org/10.1016/j.mssp.2021.106346
[35] Prabu, R. David, S. Valanarasu, V. Ganesh, Mohd Shkir, A. Kathalingam, and S. AlFaify. "Effect of spray pressure on optical, electrical and solar cell efficiency of novel Cu_2O thin films." *Surface and Coatings Technology* 347 (2018): 164-172. https://doi.org/10.1016/j.surfcoat.2018.04.084
[36] Zuo, Guangzheng, Hassan Abdalla, and Martijn Kemerink. "Impact of doping on the density of states and the mobility in organic semiconductors." *Physical Review B* 93, no. 23 (2016): 235203. https://doi.org/10.1103/PhysRevB.93.235203
[37] Sliti, Naama, Emile Fourneau, Thomas Ratz, Saâd Touihri, and Ngoc Duy Nguyen. "Mg-doped Cu_2O thin films with enhanced functional properties grown by magnetron sputtering under optimized pressure conditions." *Ceramics International* 48, no. 16 (2022): 23748-23754. https://doi.org/10.1016/j.ceramint.2022.05.028
[38] Brandt, Iuri S., Milton A. Tumelero, Cesar A. Martins, Cristiani C. Pla Cid, Ricardo Faccio, and Andre A. Pasa. "Defects controlling electrical and optical properties of electrodeposited Bi doped Cu_2O." *Journal of Applied Physics* 123, no. 16 (2018). https://doi.org/10.1063/1.5007052
[39] Jacob, S. Santhosh Kumar, I. Kulandaisamy, S. Valanarasu, A. M. S. Arulanantham, V. Ganesh, S. AlFaify, and A. Kathalingam. "Enhanced optoelectronic properties of Mg doped Cu_2O thin films prepared by nebulizer pyrolysis technique." *Journal of Materials Science: Materials in Electronics* 30 (2019): 10532-10542. https://doi.org/10.1007/s10854-019-01397-8